Non-Invasive, Real-time Assessments of the Angiogenic and Osteogenic Effects of Oxygen Releasing Scaffolds on Bone Fracture Healing with Multimodality Imaging

Yunke Ren[1], Govardhan Poondi[2], Naboneeta Sarkar[1], Jingtong Zhao[2], Allison L. Horenberg[1], Warren L. Grayson[1,2], Arvind P. Pathak[1,2]
[1]Johns Hopkins University School of Medicine, Baltimore, [2]Johns Hopkins University, Baltimore, MD
Email of presenting author: yren26@jh.edu

INTRODUCTION: Tissue-engineered oxygen-releasing scaffolds have been shown to facilitate calvarial bone healing [1-2], but our understanding of the dynamic, spatiotemporal changes they induce in the bone healing microenvironment has been limited. This is largely due to the technical challenges associated with acquiring quantitative readouts of angiogenesis and osteogenesis in vivo [3]. In this abstract, we demonstrate the feasibility of non-invasively quantifying the differential angiogenic and osteogenic effects of 3D-printed control (PCL) or oxygen-releasing scaffolds (PCL-25%CPO) in a calvarial model of bone fracture healing. We illustrate how the dynamics of bone healing can be quantified in real-time with our multimodality imaging approach.

METHODS: All animal experiments were conducted in accordance with an approved Johns Hopkins University Animal Care and Use Committee (JHU ACUC) protocol. Two 10-week-old female C57BL/6 mice (Jackson Laboratories) were anesthetized by intraperitoneal administration of ketamine (80 mg/kg) and xylazine (8 mg/kg). A 4-mm calvarial defect was created on the parietal bone of each mouse using a dental drill. Control (PCL) or oxygen-releasing (PCL-25%CPO) scaffolds (4 mm diameter × 0.4 mm thick) were implanted into the calvarial defects, and 5 mm glass coverslips used to seal the defects and permit multimodality in vivo optical imaging (**Fig. 1a-b**) consisting of Intrinsic Optical Signal (IOS) and Laser Speckle Contrast (LSC). These contrast mechanisms enabled the characterizations of structural and functional vascular changes during bone healing at high spatial (5 µm) and temporal (200 ms) resolution (**Fig. 1c-f**), and the derivation of intravascular oxygen saturation (SO_2) as described by us in [4]. Images were acquired weekly, and the vasculature was digitally segmented and processed using customized ImageJ and MATLAB algorithms. On post-surgery day 28, the mice were perfused with heparinized saline and fixed with formalin. After fixation, the skulls were harvested, and 3D micro-CT images acquired using Skyscan 1175 at 15 µm spatial resolution.

RESULTS: The cranial windows maintained their clarity over four weeks of in vivo imaging. With this multimodality optical imaging framework, we successfully characterized in vivo structural and functional vascular changes during bone healing induced by the control or oxygen-releasing scaffolds (**Fig. 2**). Week 1 data was not included in the quantifications because only dural vessels were visible and bleeding often made it challenging to reliably identify angiogenic vessels at this stage. We found that angiogenic vessels became visible during the 2nd week of bone healing and tended to wrap around the struts of the PCL and PCL-CPO scaffolds. These vessels appeared to originate either from the bony edges of the defect or from the dura mater. The angiogenic vessels exhibited larger diameters in the PCL-CPO scaffold compared to the PCL scaffold, over the 4-week healing cascade. The vessels in PCL-CPO scaffold also exhibited greater length, volume, and density than those in the PCL scaffold at Weeks 2 and 3 of healing, and during the 4th week of healing, these parameters of the vasculature decreased in the PCL-CPO scaffold but increased in the PCL scaffold, making them comparable. Blood flow within angiogenic vessels of the PCL-CPO scaffold increased and peaked at the 3rd week of healing and plateaued towards the end of the 4th week. In contrast, peak blood flow was observed at the 2nd week of healing in the PCL scaffold and continued to decrease significantly during the 4-weeks of bone healing. Interestingly, while the SO_2 of the PCL-CPO implanted defect remained at similar levels (~50%) during Weeks 2-4, the SO_2 in the PCL implanted defect continuously decreased from 70% in Week 2 to ~60% in Week 4. Finally, although no other osteoinductive factors or cells were included in the scaffolds, micro-CT images revealed improved bone healing in the PCL-CPO implanted defects (48.4%) compared to that in the PCL implanted defects (32.7%). We also observed more mineralized depositions growing further from the edges towards the middle of the defects with PCL-CPO scaffolds (**Fig. 3**).

DISCUSSION: Our multimodality in vivo imaging data demonstrated that the oxygen-releasing PCL-CPO scaffold prospectively enhanced angiogenesis during early stages of bone healing compared to PCL scaffold. While it is well-established that hypoxia is a major driving factor of angiogenesis [3], recent studies have shown that local oxygen delivery can induce robust vascular network formation by increasing endothelial cell proliferation and migration [2]. In addition, improved bone growth in the PCL-CPO implanted defects, despite its lower observed intravascular SO_2 compared to PCL implanted defects, indicates that an oxygen releasing scaffold could potentially reduce hypoxia in the bone defect microenvironment, and mitigate poor oxygen delivery from blood vessels. Based on the results of this pilot study, we are undertaking a study with a larger cohort of animals to more carefully elucidate the impact of oxygen release on bone healing. Additionally, given the observation of initially higher angiogenesis in the PCL-CPO scaffold that later converged to that in the PCL scaffold, we will evaluate bone growth at later time points to confirm if the enhanced bone formation in PCL-CPO scaffold persists at later stages of bone healing. Finally, we are working on incorporating in vivo imaging of reactive oxygen species (ROS) and local oxygen concentration into our multimodality imaging workflow to provide a more detailed characterization of the roles of cellular, molecular and systemic oxygenation changes in bone healing. In conclusion, our multimodality imaging approach enables non-invasive, real-time assessments of the angiogenic and osteogenic effects of oxygen releasing scaffolds on bone fracture healing.

SIGNIFICANCE/CLINICAL RELEVANCE: Our multimodality in vivo imaging approach holds great promise for unraveling crucial biological questions regarding the therapeutic efficacy of tissue-engineered scaffolds for treating bone fractures and advancing strategies in regenerative orthopedic research.

REFERENCES: [1] Suvarnapathaki S et. al., Bioact Mater. 2021;13:64-81; [2] Sun H et. al., Bioact Mater. 2023; 24:477-496; [3] Hankenson KD et. al., Injury. 2011;42(6):556-61; [4] Ren Y et. al., Microvascular Research. 2023; 148:104518

ACKNOWLEDGEMENTS: This work was supported by NIH/NCI grant nos. 2R01CA196701-06A1, 5R01CA237597-04 and 5R01DE027957-05.

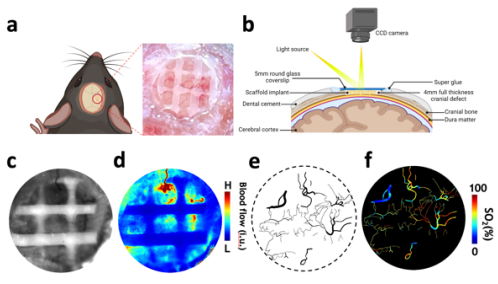

Fig. 1: Multimodality in vivo imaging of calvarial bone defect healing following scaffold implantation. (**a-b**) Illustration of the cranial window and imaging setup. Representative images of: (**c**) IOS-derived vascular structure, (**d**) LSC-derived blood flow, (**e**) segmented angiogenic vessels, and (**f**) multiwavelength IOS derived SO_2 within a calvarial defect with PCL-CPO scaffold implants at Week 4 after surgery.

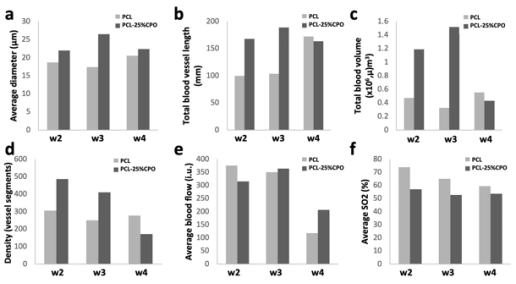

Fig. 2: Quantifications of the structural and functional vascular changes following implantation with control (gray) or oxygen-releasing (dark gray) scaffolds. Comparison of structural changes: (**a**) diameter, (**b**) total length, (**c**) total blood volume, (**d**) density. Comparison of functional changes: (**e**) blood flow, and (**f**) intravascular SO_2.

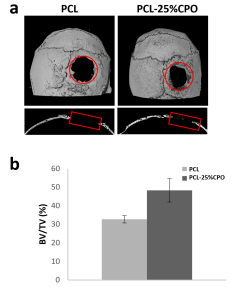

Fig. 3: Quantifications of differences in osteogenesis between animals implanted with control (gray) or oxygen-releasing (dark gray) scaffolds. (**a**) Micro-CT images of defects at post-surgery week 4. (**b**) Differences in bone growth between the two scaffolds.